Laser beam combiner for Thomson scattering core LIDAR[a)]

I. Balboa,[1,b)] B. Huang,[2] G. Naylor,[1] M. Walsh,[3] A. Sirinelli,[1] P. Parsons,[1] J. Fessey,[1] M. Townsend,[1] M. Beurskens,[1] N. Conway,[1] J. Flanagan, M. Kempenaars,[1] and A. Kirk[1]
[1]*EURATOM/CCFE Fusion Association, Culham Science Centre, Abingdon OX14 3DB, United Kingdom*
[2]*Department of Physics, University of Durham, South Road, Durham DH1 3LE, United Kingdom*
[3]*Diagnostics Division, Department of CHD, ITER Organization, CS 90 046, Bulding 155/55, Route de Vinon, 13607 Saint-Paul-Lez-Durance Cedex,France*

(Presented 17 May 2010; received 14 May 2010; accepted 31 May 2010; published online 28 October 2010)

The light detection and ranging Thomson scattering (TS) diagnostic is advantageous since it only requires a single view port into the tokamak. This technique requires a short pulse laser at high energy, usually showing a limited repetition rate. Having multiple lasers will increase the repetition rate. This paper presents a scanning mirror as a laser beam combiner. Measurements of the position accuracy and jitter show that the pointing stability of the laser beam is within ± 25 μrad for over tens of seconds. A control feedback loop is implemented to demonstrate the long term stability. Such a system could be applied for ITER and JET. © *2010 American Institute of Physics.*
[doi:10.1063/1.3485081]

I. INTRODUCTION

Thomson scattering core LIDAR (TSCL) is a diagnostic technique for measuring electron density and temperature in tokamaks.[1] This requires illuminating the plasma with a short pulse from a high power laser (e.g., ruby and Nd:YAG). Pulse widths are typically in the range of hundreds of picoseconds to tens of nanoseconds and a pulse energy values are approximately a couple of joules. A high repetition rate is also quite desirable as it enables the TS system to follow fast plasma events. However, these types of lasers have repetition rates of the order of tens of hertz. The repetition rates are mainly limited by the Q-switching process and the risk of damaging the optical components inside the laser unit.[2] It is possible to increase the repetition rate by having multiple laser units and thus interleaving the laser pulses. This involves using a laser beam combiner, which not only has to be simple, reliable, and fast but also needs to withstand the high peak energy power of these laser sources. These requirements can be met either passively with fixed optical components or actively for example with a galvanometer scanner. The main advantage of the scanner is that it can easily accommodate any number of lasers units as long as the scanning movement is within its optical range and speed performance. This paper presents a galvanometer mirror scanner as a laser beam combiner for fusion devices such as ITER and JET.

II. DESIGN SPECIFICATIONS

The LIDAR TS diagnostic at JET has successfully been running since 1986 and it is expected that a similar system will be installed at ITER. The JET LIDAR TS system only operates with a single laser, however it would greatly benefit from multiple laser operation. As for ITER, a laser repetition rate of 100 Hz is required, this means employing several lasers. Figure 1 shows pulses from N lasers incident on mirrors, which reflect the beams to a set of fixed mirrors, which direct the beams onto the scanner. The scanner sends the beams to the vessel via a rotating mirror. A second scanner has been added as contingency (see Fig. 2). In this scenario, the folding mirrors will retract and allow the beams to reach a second set of fixed mirrors, and hence to a second scanner. As an example, considering a repetition rate of 15 Hz, then seven lasers will be required to achieve a repetition rate of $\sim$100 Hz.[3] Factors affecting the choice of a suitable scanner are angular range of the mirror coating, the repetition rate, and the number of lasers which in turn determine the scanning speed and the scanning range. A scanning trajectory has been chosen which minimizes the largest change of angle in any complete sequence. Ideally, the trajectory should be such that the speed and acceleration do not show sharp discontinuities, which might affect the performance and stability of the scanning movement. For seven lasers, a trajectory considered (see Fig. 3) would be step through positions 1, 3, 5, 7, 6, 4, and 2. Translating this trajectory into angle, for a $\pm 10°$ optical scanning range, the angle between alternative laser positions will be approximately 6°. Thus, the scanning

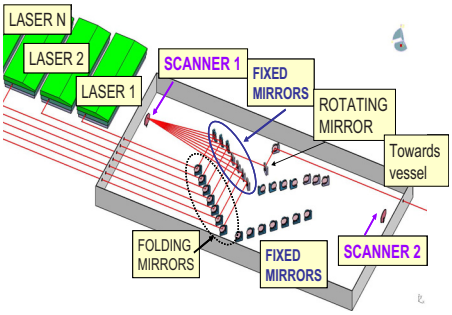

FIG. 1. (Color online) Example of layout in a TSCL system (main path).

[a)]Contributed paper, published as part of the Proceedings of the 18th Topical Conference on High-Temperature Plasma Diagnostics, Wildwood, New Jersey, May 2010.
[b)]Author to whom correspondence should be addressed. Electronic mail: itziar.balboa@ccfe.ac.uk.

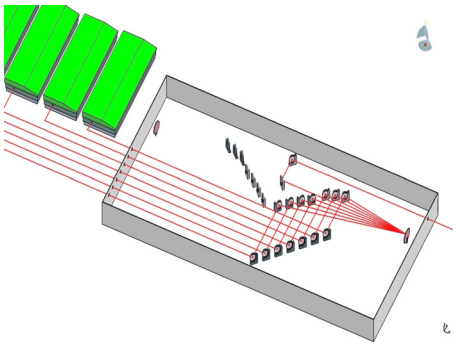

FIG. 2. (Color online) Contingency path.

speed will be deflecting the laser beam by this angle every 100 Hz, which is equivalent to 11 rad/s. The required pointing stability of the scanner is that it should be compatible with that of the laser, typically ± 25 μrad. The mirror size was based on a typical laser beam diameter for a LIDAR TS system of tens of millimeter. Table I summarizes the main parameters.

III. PROTOTYPE CONFIGURATION

To assess the performance of a galvanometer mirror scanner as a laser beam combiner a prototype has been set up which is shown schematically in Fig. 4. The main components are laser, scanner, and a quadrant photodiode (QPD) as a detector. The source is a laser diode module (class II) operating in cw. The wavelength is chosen as 650 nm for alignment purposes. The beam diameter is 4 mm. A low power laser is sufficient because the objective is to demonstrate the performance of the scanner in terms of its reliability and stability. The scanner is a galvanometer type (model M3ST, GSIG group Inc., USA), and with voltage range of ± 3 V, see Table I. The QPD (model PDQ80A, Thorlabs Ltd., UK) has a diameter of 7.8 mm, wavelength range of 400–1050 nm, output voltage of ± 2 V, and effective angular resolution of 0.3 μrad. The mirror is silver coated. The laser diode illuminates the scanner, which then reflects the beam onto the QPD. The QPD mimics the location of a second laser position. This type of detector can discriminate between vertical and horizontal displacements in beam position. The scanner is nominally shifting the between two positions along the horizontal axis. Initially, the scanner was driven by an input waveform sent by a computer (PC) via a function generator

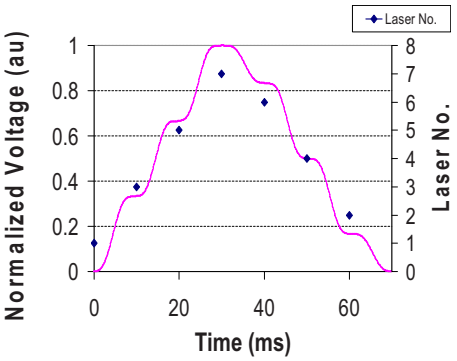

FIG. 3. (Color online) Example of input waveform for seven lasers.

TABLE I. Scanner and mirror main parameters.

Parameter	Value
Laser repetition rate	100 Hz
Scanning speed	11 rad/s ($\equiv 6°$ in <10 ms)
Scanning range	$\pm 10°$
Pointing stability	± 25 μrad
Mirror size (mm)	$55.4(w) \times 34.2(h) \times 4.06(t)$

and the QPD was connected to an oscilloscope (controlled from the same PC), for data acquisition and processing. A neutral density filter was added to avoid saturating the QPD. The distance between the laser and the scanner is 2230 ± 2 mm and the distance between the laser and the QPD is 240 ± 2 mm. The three components form a triangle where the laser beam describes a $\sim 6°$ between the QPD and the laser. This configuration was chosen for two reasons first to test the scanning speed value as explained in Sec. II and second because a relatively long distance setup will be more sensitive to position errors in the beam trajectory.

IV. HARDWARE CHARACTERIZATION

The QPD is mounted on a XYZ translation stage. By shifting the QPD position along the horizontal and vertical axes, using the translation stage, it is possible to obtain a relationship between QPD voltage and position (see Fig. 5). The voltage has been measured across the horizontal axis of the QPD, which specifically corresponds to a beam moving from left to right. The steepness is maximum in the central region which is the most sensitive area of the QPD. Therefore, it is important to ensure that the beam is aligned to hit the center of the vertical and horizontal axes. The central region has been fitted to a linear Eq. (1), where V_Q is the QPD signal voltage and D represents distance.

$$V_Q(\text{volts}) = 1.9972 \times D(\text{mm}) - 9.802. \quad (1)$$

Before assessing the scanner performance, it is necessary to measure the pointing stability for the chosen laser without the scanner to ensure that this is not a limiting factor in fulfilling the specifications.

This was carried out by using the configuration shown in Fig. 4 replacing the scanner with a fixed mirror. Measurements taken on different days over a period of 1 h with

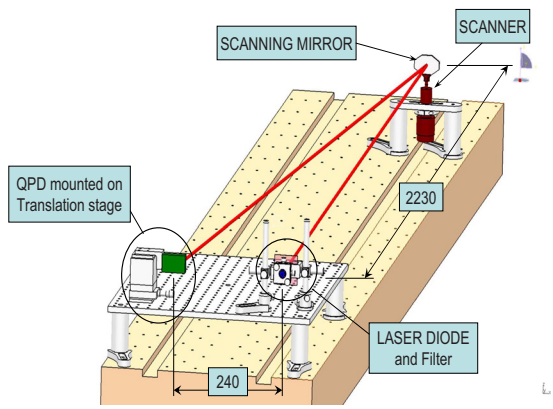

FIG. 4. (Color online) Optical layout (distances are in millimeter).

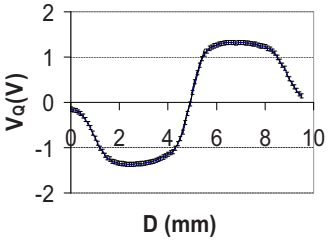

FIG. 5. (Color online) QPD calibration of voltage vs position.

measurement interval of 10 s show that the pointing stability was better than 10 μrad. For example, a typical value and standard deviation was 3.17 ± 1.12 μrad, satisfying the design specifications.

The input signal to the scanner was selected as [see Eq. (2)]

$$V_I = (t - t_0) + \frac{C}{w}\sin(w^*(t - t_0) + \phi), \tag{2}$$

where t denotes time, t_0 is the time offset, C and w are both constants, and ϕ denotes the phase. Equation (2) represents the "forward" half cycle of the scanner movement which was then reversed. The sine term corrects the first term to smooth the speed gradient at the start and stop positions. This waveform is generated by a function generator. Driving by this signal, the scanner deflects the beam to the center of the QPD and then returns the beam to its previous position. Figure 6 shows a representation of the normalized input waveform (which is symmetric about the middle point). The values for the parameters are C=−1.28, w=900, the frequency is 66.6 Hz, and the step interval is 0.1 ms. In this configuration the scanner stops for a time interval of 160 μs before reaching the tenth ms (see Fig. 7).

The QPD outputs three signals: horizontal and vertical displacements as well as the "total" contribution from all the channels. The actual displacement is obtained by normalizing each of the channels to the "total." Figure 7 shows that a

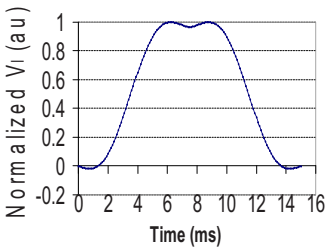

FIG. 6. (Color online) Input waveform.

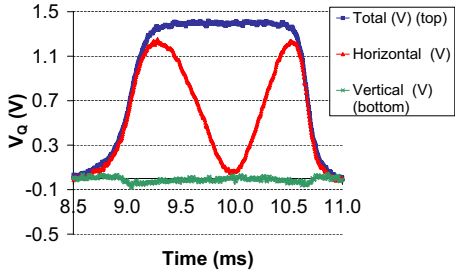

FIG. 7. (Color online) QPD signals.

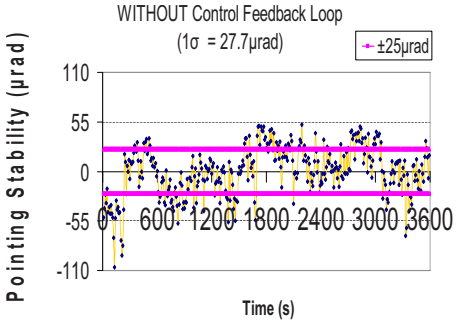

FIG. 8. (Color online) Pointing stability for 1 h (without control loop).

symmetric profile for the horizontal channel, which represents the beam arriving to the center of the QPD and returning to its previous position. The vertical channel shows zero voltage because the beam is in the center of the vertical axis.

V. PERFORMANCE ASSESSMENT

The scanner's performance has been quantified by measuring the jitter in the position of the laser beam or its pointing stability. Figure 8 shows an example of the pointing stability profile over a period of 1 h from measurements taken over a time interval of 10 s. The voltage signal was averaged over the window where the scanner stops (160 μs). From the calibration curve, it is possible to convert the voltage signal to position on the QPD and hence into angle using the triangular configuration (see Fig. 4). As shown on Fig. 8, the pointing stability of the laser beam exceeds the ± 25 μrad specifications with large fluctuations. The standard deviation is ~ 28 μrad.

Since the type of behavior is inadequate, a control feedback loop has been added to extend the stability to longer time scales. The frequency spectrum associated with Fig. 8 is shown in Fig. 9, exhibiting a 1/f noise profile where the broadband noise floor is reached at ~ 0.005 Hz. This indicates the frequency range at which the control feedback loop will have to operate.

VI. CONTROL FEEDBACK LOOP: STABILITY

To ensure stability performance can be maintained on a long term basis, a control feedback loop was implemented, modifying then the initial layout. The scanner was driven from a field-programmable gate array (FPGA) board (Nexys II, Digilent Inc., USA) and the QPD signal was processed by

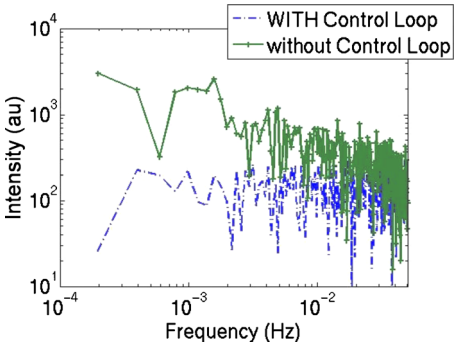

FIG. 9. (Color online) Frequency spectrum with and without control loop.

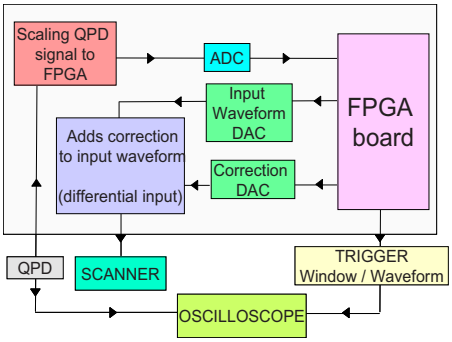

FIG. 10. (Color online) Schematic of the control loop.

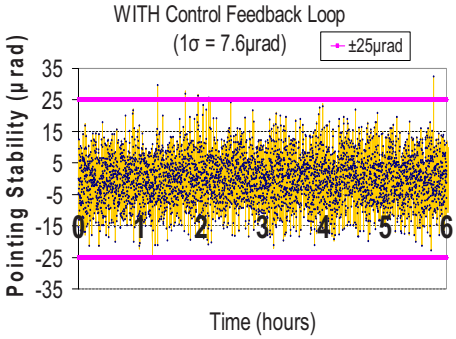

FIG. 12. (Color online) Pointing stability WITH control feedback loop for 6 h.

the FPGA board. The correction to the input waveform to keep the pointing stability within its specified range was then determined. The correction is an offset added to the input signal. A simple three option algorithm was implemented for the correction: when the beam is pointing at the center of the QPD, there is no correction, when the average voltage is between ±50 and ±100 mV, which corresponds to a pointing stability of ±12.5 to ±25 μrad, the correction is ±0.014 mV. Outside this range, the correction is ±0.14 mV. Figure 10 shows a schematic of the control loop and the entire setup. The FPGA has three peripheral boards: two digital to analog converters (DACs) of 12 bits per channel (two channels) and one analog to digital converter (ADC 2 12 bits). The ADC board is connected to a board which scales the signal from the QPD to the FPGA range. The two DACs are connected to a board which combines the main waveform with the correction and sends that signal to the scanner. A second detector, illuminated from a beam splitter, was added to the setup to confirm the measurements from the first detector (see Fig. 11). Figure 12 shows the pointing stability measured over a period of 6 h. The data sampling is 5 s, which gives a total of ~4400 data points. The standard deviation is 7.6 μrad, a factor of 3 over the configuration without feedback. There are a few outliers but even the largest is less than 35 μrad, which is still tolerable. The control feedback loop meets its specifications to a three-sigma level. The associated frequency spectrum (see Fig. 9) shows that the residual noise is flat across frequency and has, as a result, improved the stability of the device.

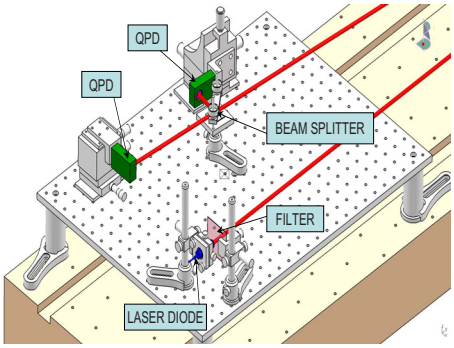

FIG. 11. (Color online) Detail of the prototype layout with two detectors.

ACKNOWLEDGMENTS

This work is funded jointly by the United Kingdom Engineering and Physical Sciences Research Council under Grant No. EP/G003955 and the European Communities under the contract of Association between EURATOM and CCFE. The views and opinions expressed herein do not necessarily reflect those of the European Commission and of the ITER organization.

[1] H. Salzmann, J. Bundgaard, A. Gadd, C. Gowers, V. Gusev, K. B. Hansen, K. Hirsch, P. Nielsen, K. Reed, C. Schrodter, and K. Weisberg, "The LIDAR Thomson scattering diagnostic on JET," EFDA-JET Report No. JET-T(89)07, 1989.
[2] W. Koechner, *Solid-State Laser Engineering*, 6th ed. (Springer-Verlag, Berlin, Germany, 2006).
[3] M. J. Walsh, M. Beurskens, P. G. Carolan, M. Gilbert, M. Loughlin, A. W. Morris, V. Riccardo, and Y. Xue, Rev. Sci. Instrum. **77**, 10E525 (2006).